

Exposure Disparities by Income, Race and Ethnicity, and Historic Redlining Grade in the Greater Seattle Area for Ultrafine Particles and Other Air Pollutants

Kaya Bramble,¹ Magali N. Blanco,² Annie Doubleday,² Amanda J. Gassett,² Anjum Hajat,³ Julian D. Marshall,⁴ and Lianne Sheppard^{2,5}

¹Department of Industrial & Systems Engineering, College of Engineering, University of Washington, Seattle, Washington, USA

²Department of Environmental and Occupational Health Sciences, School of Public Health, University of Washington, Seattle, Washington, USA

³Department of Epidemiology, School of Public Health, University of Washington, Seattle, Washington, USA

⁴Department of Civil & Environmental Engineering, College of Engineering, University of Washington, Seattle, Washington, USA

⁵Department of Biostatistics, School of Public Health, University of Washington, Seattle, Washington, USA

BACKGROUND: Growing evidence shows ultrafine particles (UFPs) are detrimental to cardiovascular, cerebrovascular, and respiratory health. Historically, racialized and low-income communities are exposed to higher concentrations of air pollution.

OBJECTIVES: Our aim was to conduct a descriptive analysis of present-day air pollution exposure disparities in the greater Seattle, Washington, area by income, race, ethnicity, and historical redlining grade. We focused on UFPs (particle number count) and compared with black carbon, nitrogen dioxide, and fine particulate matter (PM_{2.5}) levels.

METHODS: We obtained race and ethnicity data from the 2010 U.S. Census, median household income data from the 2006–2010 American Community Survey, and Home Owners' Loan Corporation (HOLC) redlining data from the University of Richmond's Mapping Inequality. We predicted pollutant concentrations at block centroids from 2019 mobile monitoring data. The study region encompassed much of urban Seattle, with redlining analyses restricted to a smaller region. To analyze disparities, we calculated population-weighted mean exposures and regression analyses using a generalized estimating equation model to account for spatial correlation.

RESULTS: Pollutant concentrations and disparities were largest for blocks with median household income of <\$20,000, Black residents, HOLC Grade D, and ungraded industrial areas. UFP concentrations were 4% lower than average for non-Hispanic White residents and higher than average for racialized groups (Asian, 3%; Black, 15%; Hispanic, 6%; Native American, 8%; Pacific Islander, 11%). For blocks with median household incomes of <\$20,000, UFP concentrations were 40% higher than average, whereas blocks with incomes of >\$110,000 had UFP concentrations 16% lower than average. UFP concentrations were 28% higher for Grade D and 49% higher for ungraded industrial areas compared with Grade A. Disparities were highest for UFPs and lowest for PM_{2.5} exposure levels.

DISCUSSION: Our study is one of the first to highlight large disparities with UFP exposures compared with multiple pollutants. Higher exposures to multiple air pollutants and their cumulative effects disproportionately impact historically marginalized groups. <https://doi.org/10.1289/EHP11662>

Introduction

Long-term exposure to air pollution is associated with adverse health effects, such as cardiovascular and respiratory diseases and cognitive decline.^{1–3} Historically, racialized groups and low-income communities have been more likely to be exposed to higher concentrations of air pollution, contributing to health disparities.^{4–13} Many different factors can affect health outcomes, and it has been well documented that life expectancy, morbidity, and mortality in the United States varies based on income level, race and ethnicity, and residential location.^{14–19}

Disparities in environmental health in the United States are a result of structural racism, including ongoing and historic segregation and urban planning decisions. For example, starting in the 1930s, the Home Owners' Loan Corporation (HOLC) graded residential areas by “mortgage security” on an A-to-D scale: “A” indicated the lowest financial risk to lenders that borrowers would default on mortgage loans and “D” indicated highest risk to lenders. Several factors, such as closeness to transportation, amenities, or industry presence, also contributed to grading.²⁰

Racial, ethnic, and religious composition were significant contributing factors to a neighborhood's grade, allowing lenders to reduce the accessibility of mortgage financing for people of color and immigrants.²¹ The HOLC's maps depicted Grade D in a red color, and this grading practice became known as redlining. HOLC grades were delineated decades ago, yet they correlate with present-day social and environmental attributes of neighborhoods.^{22–25} In addition, “racial covenants” on homes and neighborhoods established and enforced “White only” communities, resulting in further racial residential segregation.²⁶ Furthermore, zoning regulation, the barriers to homeownership faced by Black people as a result of discriminatory lending practices, the continual lack of enforcement by government officials in the face of discriminatory practices, and placement of polluting activities such as highways and industry, into communities of color all reinforced residential segregation, which resulted in higher exposure to environmental hazards among these communities.²⁶ Historically, and still today, racialized and low-income communities generally have fewer health-promoting resources to adequately address the health effects of air pollution, including less access to amenities such as green-spaces and health care facilities, maintaining the health disparities created by structural racism.²⁷ When racism or classism impede the right to a healthy living environment, including the air we breathe, this is an environmental injustice.

Ultrafine particles (UFPs) are particles suspended in air with aerodynamic diameters of <100 nm. As a result of their small size, UFPs can pass through the blood–air barrier in the lungs that transfers oxygen to blood.²⁸ Growing evidence suggests that UFPs can also cross the blood–brain barrier, which serves to protect the brain from toxins and pathogens.²⁹ UFPs are composed of toxic metals and compounds that have been associated with adverse heart, lung, and brain health effects.²⁸ UFPs are emitted

Address correspondence to Lianne Sheppard, Hans Rosling Center for Population Health, Box 351618, 3980 15th Ave. NE, Seattle, WA 98195 USA. Email: sheppard@uw.edu

Supplemental Material is available online (<https://doi.org/10.1289/EHP11662>).

The authors declare they have nothing to disclose.

Received 2 June 2022; Revised 15 May 2023; Accepted 1 June 2023; Published 5 July 2023.

Note to readers with disabilities: *EHP* strives to ensure that all journal content is accessible to all readers. However, some figures and Supplemental Material published in *EHP* articles may not conform to 508 standards due to the complexity of the information being presented. If you need assistance accessing journal content, please contact ehpsubmissions@niehs.nih.gov. Our staff will work with you to assess and meet your accessibility needs within 3 working days.

by transportation and other sources of fossil fuel combustion.^{28,30} In most ambient urban environments, UFPs dominate particle numbers but weigh very little and thus contribute nearly zero to the regulatory mass-based measurements for fine particulate matter [PM_{≤2.5} μm in aerodynamic diameter (PM_{2.5})].³⁰ This is why UFPs are often measured as particle number count (PNC).

Limited existing research has explored UFP exposure disparities by race and ethnicity, income, or redlining grade. Chambliss et al. compared nitric oxide (NO), nitrogen dioxide (NO₂), black carbon (BC), and UFP exposure disparities between different races and ethnicities in the San Francisco Bay area.⁵ The authors measured pollutants by mobile monitoring, and they found median concentrations of NO, NO₂, and UFPs to be higher for Hispanic and Black populations and lower for White populations in their study region. Saha et al. studied UFP disparities by race and ethnicity and income across the United States, and found 35% higher than average concentrations for Asian, Black, and Hispanic populations.⁶ Other observational studies on air pollution exposure disparities by race, ethnicity, and socioeconomic status have focused on criteria pollutants, such as NO₂, PM_{2.5}, and ozone (O₃) across the United States; most have found higher pollution levels in low-income and racialized communities.^{7–13} Previous studies have also examined the association of redlining grade with BC, NO₂, and PM_{2.5}, and found that pollutant concentrations increased with less desirable HOLC grades.^{31–34} Other studies examining the health or environmental effects of redlining have found an association with asthma, lack of health insurance, and reduced present-day greenspace with more hazardous HOLC grades.^{24,35–37}

Through the Clean Air Act,³⁸ the U.S. Environmental Protection Agency (EPA) sets national standards for six criteria air pollutants, including O₃, NO₂, and PM, all of which have been shown to harm health. These pollutants have been monitored continuously at >4,000 monitoring stations operated by states and local agencies throughout the country.³⁹ Although some states choose to monitor UFPs, there is a lack of long-term and widespread UFP monitoring.⁴⁰ At this time, there is no standard metric of measurement for UFPs. PNC is the most commonly used metric, but concentrations vary owing to differences across instruments in the range of the particle sizes they measure and in their efficiency in counting particles.⁴⁰ Few studies have examined disparities of UFPs and other noncriteria air pollutants, such as BC, despite increasing evidence that these pollutants are also associated with adverse health effects.^{41–43} Similarly, to the best of our knowledge, no studies have considered disparities associated with redlining grade and UFPs.

The primary aim of this paper was to examine how contemporary income, race and ethnicity, and historic redlining grade impact present-day UFP exposure disparities in the Seattle, Washington, area. We compared UFP exposures between income groups, racial and ethnic groups, and redlining grade to see how much pollutant concentrations must decrease to make groups with the highest exposures comparable to those with the lowest. The disparities by redlining grade show the lasting effects of discriminatory urban planning practices, whereas the disparities by present-day income and race and ethnicity reflect both the ongoing impacts of racist policies and the modern populations that are disproportionately affected. Further, in descriptive analyses, we estimated magnitudes of difference in pollutants between HOLC Grade A and more hazardous grades and examined how accounting for income and race and ethnicity impacts these estimated differences. We additionally considered how these disparities relate to BC, NO₂, and PM_{2.5} exposure levels and compared relative disparities across pollutants to put our study results into context with previous studies and identify the potential for cumulative health effects for groups disproportionately exposed to

multiple pollutants. With the current lack of research on UFP disparities, this paper will help inform future research and regulation to prevent detrimental health effects.

Methods

Study Region

Our analyses used demographic data from the 2010 U.S. Census⁴⁶ and the American Community Survey (ACS),⁴⁵ aggregated from 2006–2010, as well as predicted pollutant concentrations obtained by mobile monitoring.⁴⁴ The study region was defined as the parts of Seattle represented by these mobile monitoring data (Figure 1). The unit of analysis was the census block, specifically any populated census blocks that fell completely within the modeling region.

Demographic and Redlining Data

Our primary demographic variables were median household income and race and ethnicity. We obtained income from the U.S. Census Bureau's ACS, aggregated from 2006–2010, available as a continuous variable at the block group level.⁴⁵ We obtained race and ethnicity percentages from the 2010 U.S. Census, available at the block level.⁴⁶ These data were the most recently available at the time our mobile monitoring campaign was conducted. We applied block group incomes to each of the blocks contained within the group. Of 21,535 total blocks with nonzero population in the study region, 109 blocks without households (i.e., zero residential population; 0.5% of blocks and 0.3% of population) and an additional two blocks without household income data (0.01% of blocks and 0.2% of population) were excluded from the analysis, leaving 21,424 total blocks (1,914,992 people). We focused on six race and ethnicity categories: Asian, Black, Hispanic, Native American, non-Hispanic White, and Pacific Islander. Although the non-Hispanic White category excludes all Hispanic individuals, the race (Asian, Black, Native American, and Pacific Islander) and ethnicity (Hispanic) categories are not necessarily mutually exclusive, but the degree of overlap between categories was minimal. Owing to low population numbers, results for Native Americans and Pacific Islanders should be interpreted with caution (Table 1).

We obtained redlining data for Seattle from the Mapping Inequality project from the University of Richmond's Digital Scholarship Lab.²¹ Based on a map created by the HOLC in 1936, the HOLC delineated and graded 60 areas in Seattle. Only areas that were primarily residential received a grade. The grades were characterized as “best” (A), “still desirable” (B), “declining” (C), and “hazardous” (D). Within the broader HOLC-graded region, some areas were not primarily residential but were, rather, deemed industrial or business at the time and were left ungraded. We drew a boundary around the HOLC-graded region and assigned the blocks that fell within the ungraded region grade “X.” We included these ungraded areas in our study because some do have a population today, a population that notably has the lowest median income among the HOLC grades (Table 1). Further, because these areas were deemed industrial, remaining industrial infrastructure may affect exposure levels given that they are potential sources of air pollution.

Of the ~1,200 km² covered by the mobile monitoring study region, ~1,020 km² were covered by the 21,424 included census blocks. For the redlining analysis, we categorized these blocks by the HOLC-graded areas they intersected with. This included 6,359 blocks covering 119 km², with 7.8 km² of blocks assigned to Grade A, 49.6 km² to Grade B, 37.4 km² to Grade C, and 24.1 km² to Grade D. Eighty-five percent of these blocks intersected with only one HOLC grade, and 15% of the blocks

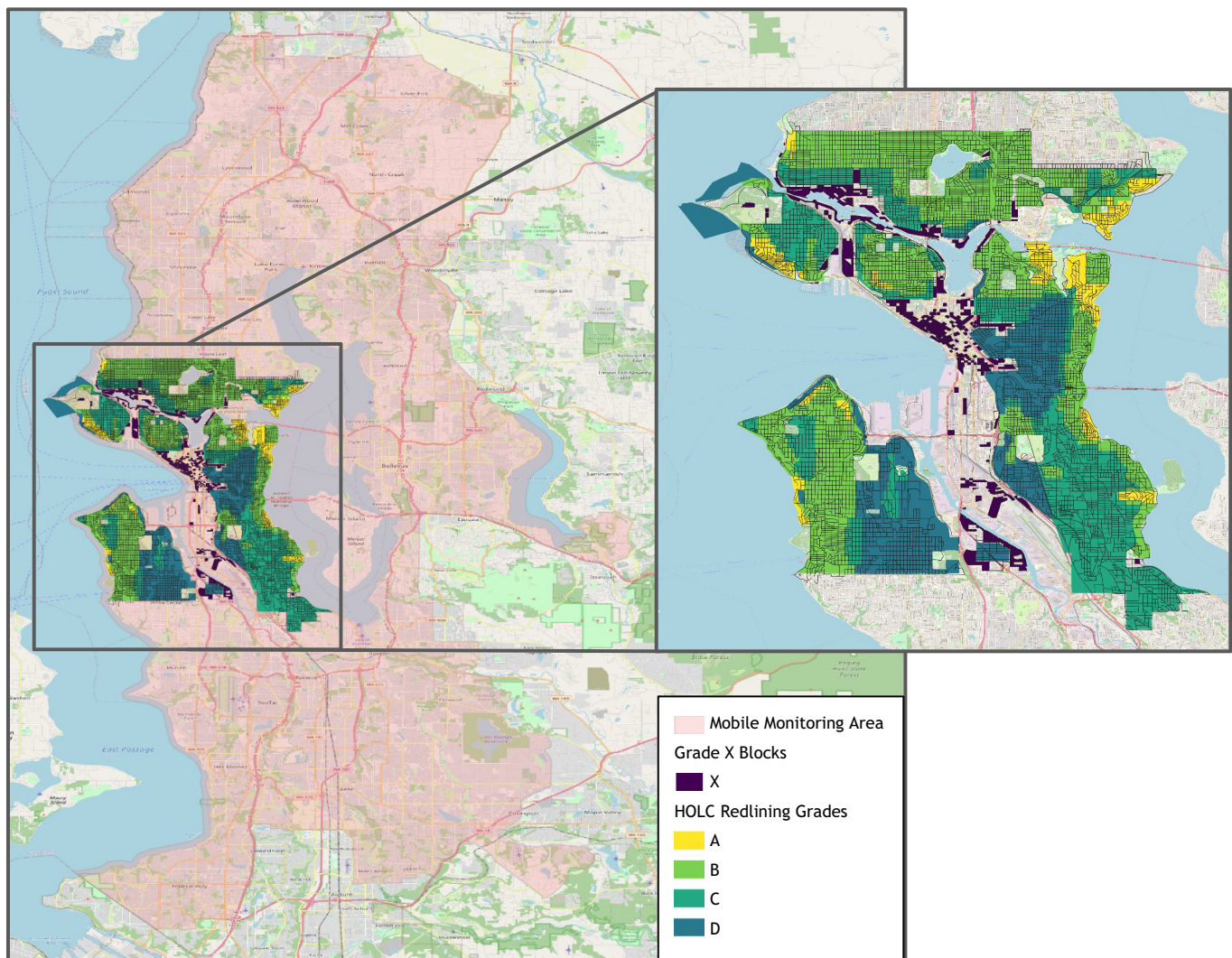


Figure 1. Seattle study region with Home Owners' Loan Corporation (HOLC) redlining grades, from A ("best") to D ("hazardous") and X ("interior uncategorized"). Areas within the HOLC-graded region that do not show any blocks are areas without residential population in the 2010 U.S. Census. Maps were generated in Quantum Geographic Information System (QGIS) using data from the American Community Survey (ACS),⁴⁵ the 2010 U.S. Census,⁴⁶ and the University of Richmond's Mapping Inequality.²¹

($n = 933$) intersected with and were split among multiple grades, such that an even share of the block's population was attributed to each grade. There were 492 populated blocks within the ungraded interior region covering 7.9 km² and assigned to grade X. Blocks were only included as Grade X if no part of the block intersected with a graded area and if the block fell completely within the interior region (Table 1, Figure 1; a version of Figure 1 that depicts traditional HOLC colors is available as Figure S1). Maps were generated in Quantum Geographic Information System (QGIS), using data from the ACS, the U.S. Census, and the University of Richmond's Mapping Inequality.

Air Pollution Data

We obtained air pollution data from a year-long mobile monitoring campaign that measured multiple pollutants simultaneously during 288 d between March 2019 and March 2020.⁴⁴ Measurements were taken from nine fixed routes during all seasons, days of week, and most times of day to maximize sampling temporality and under a balanced design to target unbiased annual average estimates.⁴⁴ Measurement days covered a median 112-km driving distance over 5.2 h, comprising 4.1 h of driving plus 1.1 h of short-term

(2-min) stops at near-roadway locations. An average of 29 valid 2-min measurements were collected from each stop. UFP concentrations were measured as PNC for particles >20 nm (P-TRAK 8525; TSI, Inc.). BC was measured by light absorption (AethLabs MA200), whereas NO₂ was measured by the Aerodyne Research Inc. CAPS NO₂ monitor. PM_{2.5} was measured as light scattering by a nephelometer (Radiance Research M903) and converted to mass using a calibration equation.⁴⁴ Roadside stop locations included 304 residential locations, and 5 regulatory monitoring locations.⁴⁴ Given the intentionally balanced design, stop-level annual averages were estimated by an unadjusted average of the win-sorized 2-min measurement medians.

Separate prediction models were developed for each pollutant: UFP (PNC), BC, NO₂, and PM_{2.5}. Geographic covariate predictors with sufficient variability and limited outliers among the monitoring locations were selected from 350 candidate covariates. The 191 selected variables were collapsed using the first three components from partial least squares regression, and they were used as covariates in universal kriging prediction models.⁴⁴ Overall, the models showed good predictive performance with a cross-validated R^2 of 0.77 for UFP, 0.60 for BC, 0.77 for NO₂, and 0.70 for PM_{2.5}.⁴⁴ It is notable that, although the mobile

Table 1. Median and IQR for air pollution and demographic data in the greater Seattle study region and Home Owners' Loan Corporation (HOLC)-graded region at the block level.

	Blocks (N)	People (N)	Populated area (km ²)	UFP (pt/cm ³)	BC (ng/m ³)	NO ₂ (ppb)	PM _{2.5} (µg/m ³)	Income (\$1,000)	Asian (%)	Black (%)	Hispanic (%)	Native American (%)	Non-Hispanic White (%)	Pacific Islander (%)
Study region														
Total area	21,424	1,914,992	1,020	6,440 (5,530–7,700)	513 (446–599)	8.6 (7.4–9.9)	4.6 (4.2–5.0)	73 (55–96)	8 (2–19)	1 (0–6)	4 (0–10)	0 (0–0)	74 (55–86)	0 (0–0)
HOLC-graded region (Grades A–D, X)	6,851	478,541	127	7,620 (6,760–8,500)	588 (517–661)	10.3 (9.2–11.8)	5.0 (4.7–5.3)	70 (54–97)	6 (2–14)	1 (0–8)	4 (0–7)	0 (0–0)	79 (59–88)	0 (0–0)
Outside HOLC-graded region	14,573	1,436,451	893	5,910 (5,220–6,960)	480 (426–557)	7.9 (6.9–8.9)	4.4 (4.1–4.7)	74 (56–97)	10 (2–20)	0 (0–6)	4 (0–11)	0 (0–0)	71 (54–84)	0 (0–0)
HOLC-graded region														
A	486 (230 split ^a)	15,884	7.8	7,380 (6,540–7,750)	545 (516–587)	9.1 (8.6–9.8)	4.8 (4.7–5.0)	112 (97–145)	3 (0–8)	0 (0–2)	0 (0–4)	0 (0–0)	88 (81–95)	0 (0–0)
B	3,449 (752 split)	188,178	49.6	7,030 (6,310–7,740)	577 (503–633)	10.0 (8.9–11.5)	5.0 (4.6–5.3)	81 (64–107)	5 (1–9)	0 (0–3)	3 (0–6)	0 (0–0)	84 (75–91)	0 (0–0)
C	2,228 (679 split)	145,150	37.4	7,890 (6,990–8,500)	594 (531–654)	10.3 (9.3–11.2)	5.0 (4.8–5.3)	62 (51–78)	8 (4–24)	3 (0–17)	4 (0–8)	0 (0–0)	74 (35–84)	0 (0–0)
D	1,116 (242 split)	83,986	24.1	8,900 (8,040–10,060)	582 (511–694)	11.0 (9.9–12.8)	4.7 (4.4–4.9)	59 (43–69)	11 (4–27)	9 (2–20)	6 (2–13)	0 (0–1)	52 (31–70)	0 (0–0)
X	492	45,343	7.9	11,800 (8,830–13,480)	884 (825–959)	15.3 (13.5–18.6)	5.6 (5.3–5.8)	50 (36–60)	6 (0–14)	1 (0–6)	5 (0–8)	0 (0–1)	74 (58–86)	0 (0–0)

Note: The median (IQR) block population was 54 (31–97) people. BC, black carbon; IQR, interquartile range; NO₂, nitrogen dioxide; PM_{2.5}, fine particulate matter; pt, particles; UFP, ultrafine particles. ^aBlocks that fall between multiple HOLC grades contribute evenly to the total population, proportionally to the populated area, and are included in the median and IQR for the other items (labeled as "split").

monitoring campaign measured PM_{2.5}, the region's low concentrations occasionally resulted in noisy readings near the instrument's limit of detection and thus some unstable readings. Predictions for each pollutant were generated at block centroids.

Exposure Disparities

We calculated the population-weighted mean air pollution concentrations for nine income categories (\leq \$20,000, \$20,000–\$40,000, \$40,000–\$50,000, \$50,000–\$60,000, \$60,000–\$70,000, \$70,000–\$80,000, \$80,000–\$90,000, \$90,000–\$110,000, $>$ \$110,000), for each race and ethnicity category (Asian, Black, Hispanic, Native American, non-Hispanic White, Pacific Islander), and for each HOLC grade (A, B, C, D, X). Income categories were selected such that each break contained a similar number of blocks, except for the $<$ \$20,000 income group, which contained fewer blocks but was highlighted to show disparities for the lowest-income households. The population-weighted means were calculated using the weighted.mean() function of the stats package (version 4.2.2) in R (version 4.2.2; R Development Core Team). For the income analysis, the block group-level income was first applied to each block, and the block centroid air pollution prediction was weighted by the block population. The mean air pollution for each income category is the weighted average of the relevant predictions:

$$\frac{\sum(\text{number of people in block } i) \times (\text{pollutant concentration in block } i)}{\text{total number of people in income category } k} \quad (1)$$

For race and ethnicity, the block centroid prediction was weighted by the subset of the block-level population identifying as that race and ethnicity:

$$\frac{\sum(\text{number of people of race or ethnicity } k \text{ in block } i) \times (\text{pollutant concentration in block } i)}{\text{total number of people of race or ethnicity } k} \quad (2)$$

For HOLC grade, the mean was an average of block centroid predictions weighted by the total populations of each block within that HOLC grade:

$$\frac{\sum(\text{number of people in block } i) \times (\text{pollutant concentration in block } i)}{\text{total number of people in HOLC grade } k} \quad (3)$$

If a block was split between multiple grades, an even share of the population was attributed to each grade.

There were many options as to how we could define our HOLC-graded area when creating our study design. To ensure that dividing the population evenly, as opposed to another method, did not meaningfully affect results, we conducted two sensitivity analyses to determine *a*) how including or excluding the blocks that fall under multiple grades affected the results (Table S1), and *b*) how splitting the block population evenly or weighing the split by the area assigned to the grade affected the results (Table S2). We additionally conducted a sensitivity analysis by recreating the main results of the paper with the data restricted to the HOLC-graded area. However, because the redlining area was restricted to an urban area of Seattle, exposure for people living in suburbs was better represented by the overall study area.

To further examine air pollution exposure disparities, we created separate population-weighted linear regression models to describe present-day disparities by how much exposures would need to change to make the groups with the highest exposure and groups with the lowest comparable. The block centroid pollutant

predictions were the outcome, and our present-day demographic variables were the predictors. In the first, we used the \log_{10} -transformed block group-level median household income applied to each block to produce an approximately linear relationship. Similarly, to examine disparities by race and ethnicity, we fit separate models for each race and ethnicity group using the block-level percentages of that group. We restricted these analyses to the four largest population groups (Asian, Black, Hispanic, non-Hispanic White). For each regression model, we qualitatively compared the linear model fit to a data smoother using visual inspection. The data smoother was created using the `geom.smooth()` function of the `ggplot2` package (version 3.4.1) in R to assess the linearity of the model. In a final set of analyses restricted to the HOLC-graded region, we conducted two population-weighted regression analyses to see whether disparities differed when considering historic HOLC grades and present-day demographics: *a*) with HOLC grade alone, and *b*) with HOLC grade adjusted for median household income (\log_{10} -transformed) and non-Hispanic White block population percentage. For this analysis, we subtracted $\log(\$117,134)$ from income and 85.8% from the non-Hispanic White percentage such that the intercept in this analysis is the mean exposure for a block with HOLC Grade A, 85.8% non-Hispanic White, and \$117,134 average income. This allows the intercept estimates for the single and multiple regressions to be more comparable. For all regression analyses, we also adjusted for spatial correlation in the data, using a generalized estimating equation (GEE) model with an identity link. This GEE approach is equivalent to the restricted spatial GEE estimate described by Hui and Bondell.⁴⁷ These parameter estimates maintain all the variation associated with the covariates in the marginal mean model while accounting for the remaining spatial correlation in the standard error estimates. We fit the GEE model using the `geeglm()` function from the `geepack` package (version 1.3.9) in R.

Results

Study Region and Data Summaries

The study region consisted of 21,424 blocks that had nonzero household population and income data and fell within the mobile monitoring region; this study region included much of the urban core in the greater Seattle metropolitan area, comprising 1,914,992 people as of the 2010 U.S. Census.⁴² Demographic and exposure data are summarized in Table 1. Notably, with medians of $4.6 \mu\text{g}/\text{m}^3$ and 8.6 ppb for $\text{PM}_{2.5}$ and NO_2 , respectively, air pollution levels were low for our study region in comparison with other urban areas in the United States and for the U.S. EPA annual standards of $12.0 \mu\text{g}/\text{m}^3$ for $\text{PM}_{2.5}$ and 53 ppb for NO_2 .⁴⁸ $\text{PM}_{2.5}$ also had little variation, with the interquartile range for the study region being $4.2\text{--}5.0 \mu\text{g}/\text{m}^3$. The most highly correlated pollutants were NO_2 and BC ($r = 0.91$), and the pollutants with the lowest correlation were $\text{PM}_{2.5}$ and UFP ($r = 0.48$). The correlations between other pollutants were between 0.70 and 0.81: BC and UFP ($r = 0.81$), NO_2 and UFP ($r = 0.81$), BC and $\text{PM}_{2.5}$ ($r = 0.73$), and NO_2 and $\text{PM}_{2.5}$ ($r = 0.70$).

Analysis of the 2010 U.S. Census data indicates that, our study region was predominantly non-Hispanic White, at a median of 74% per block and a median of 8% Asian, 4% Hispanic, and 1% Black per block. Within the HOLC-graded region, HOLC Grade A had a median of 88% non-Hispanic White, which decreased to 52% for Grade D (Table 1). HOLC Grade A had a median of 3%, 0%, and 0% Asian, Black, and Hispanic per block, respectively, which increased to 11%, 9%, and 6% in Grade D. Similarly, median household income decreased from \$112,000 to \$59,000 between grades A and D. The demographics in our Grade X were between grades B and C in percentage of Asian, Black, and non-Hispanic White population and between grades C

and D in percentage of Hispanic population. The Grade X median income (\$50,000) was the lowest of all the grades. Finally, the median pollutant concentrations in the HOLC-graded regions were higher than the rest of the study region given that the HOLC-graded region was in the urban core of Seattle and did not include suburban areas. Many of the blocks with lower income and a lower percentage of non-Hispanic White population were in the southern part of the study region (Figure 2).

Exposure Disparities by Income

Table 2 gives the population-weighted pollutant means by income group. The table suggests that the largest disparities were for NO_2 , followed by UFP, BC, and $\text{PM}_{2.5}$, by magnitude of percentage difference relative to the study region average concentration. Each pollutant showed a meaningfully higher exposure in the lowest income group of $<\$20,000$. When comparing population-weighted means, NO_2 had the strongest disparity for the $<\$20,000$ group; UFP disparities were larger relative to the study region average in the remaining categories. For UFP, the population-weighted mean exposure was $1,990 \text{ pt}/\text{cm}^3$ (22%) higher for blocks with a median household income of $<\$20,000$ compared with blocks with a median household income of between \$20,000 and \$40,000. In turn, blocks in the \$20,000–\$40,000 income range had exposure levels $1,300 \text{ pt}/\text{cm}^3$ (18%) higher than the study region average.

In the population-weighted, unadjusted linear regression model with \log_{10} -transformed median household income as the predictor variable, UFP concentration decreased by $183 \text{ pt}/\text{cm}^3$ [95% confidence interval (CI): 169, 197] for every 10% increase in income. BC concentration decreased by $11.3 \text{ ng}/\text{m}^3$ (95% CI: 10.6, 12.0), and NO_2 by 0.21 ppb (95% CI: 0.20, 0.22), for every 10% increase in income (Table S3). The increase for $\text{PM}_{2.5}$, although statistically significant, is small. The \log_{10} -transformation of median household income resulted in a more linear trend in the data. When comparing the linear model to a data smoother, there was a deviation from linearity for the highest incomes, namely, $>\$100,000$, where the regression estimated a lower exposure than the smoother (Figure S2). In addition, for NO_2 , there was a deviation for the lowest incomes, namely, $<\$30,000$, where the regression again estimated a lower exposure than the smoother.

Exposure Disparities by Race and Ethnicity

Table 3 gives the population-weighted pollutant means by racial and ethnic group. For UFP, the average exposure for non-Hispanic White residents in the study region was the lowest at $6,450 \text{ pt}/\text{cm}^3$ and the highest for Black residents at $7,740 \text{ pt}/\text{cm}^3$. This trend was reflected in BC and NO_2 as well, with non-Hispanic White residents experiencing the lowest concentrations and Black residents experiencing the highest. There were disparities for the Hispanic, Native American, and Pacific Islander residents for UFPs and BC. However, UFP had a notably higher percentage difference when comparing racialized groups to the overall average, indicating a larger disparity. $\text{PM}_{2.5}$ showed slight variation between all racial and ethnic groups.

Figure 3 (and the corresponding Table S4) shows the mean increase in pollutant concentrations and their 95% CIs for a 5% increase in racial and ethnic percentage in linear regression models fit separately by racial and ethnic group. There was a general pattern across all pollutants that mean exposure decreased as the percentage of non-Hispanic White population increased, whereas mean exposure increased as the percentage of Black and Hispanic population increased. For Asian residents, an increase in the percentage of this population was associated with a decrease in $\text{PM}_{2.5}$ and an increase in UFPs, BC, and NO_2 . Qualitatively, comparing the regression model to a data smoother, the trend for non-

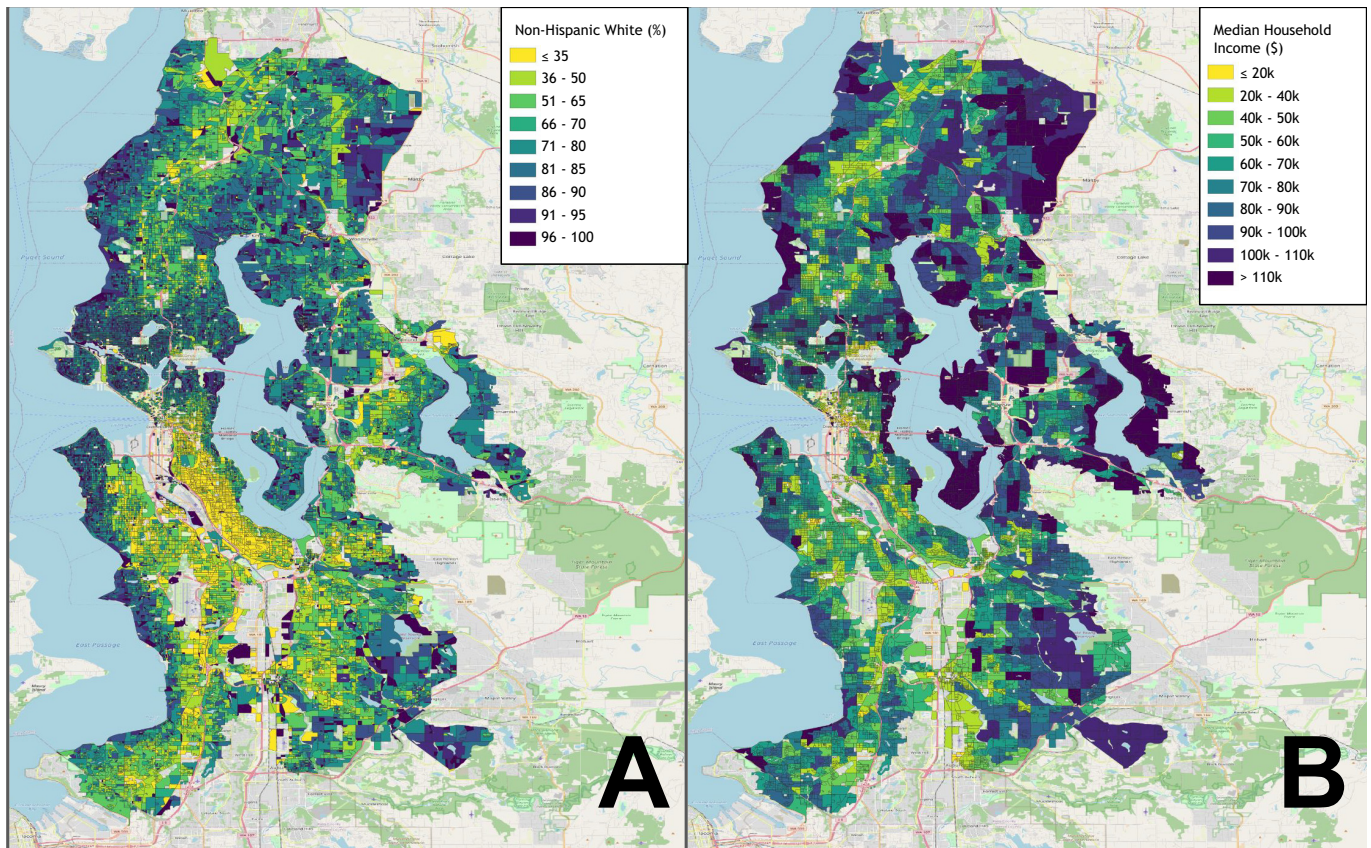


Figure 2. Distribution of (A) non-Hispanic White percentage from the 2006–2010 American Community Survey (ACS)⁴⁵ and (B) median household income from the 2010 U.S. Census⁴⁶ for blocks with household population in the study region. Legend breaks were selected such that each break contains a similar number of blocks, except for the <\$20,000 income group, which contained fewer blocks but was highlighted owing to large disparities. Note: k, thousand.

Hispanic White residents was linear throughout for each pollutant (Figure S3). The trend was also linear for Hispanic residents, but the regression estimated a higher exposure than the smoother for UFPs for the blocks with population percentages >50% (0.01% of data) (Figure S4). For Black residents, the regression model estimated a higher exposure for the blocks with percentages >35% (0.03% of data) (Figure S5). The regression model estimated a lower exposure for Asian residents for the blocks with percentages >50% (0.1% of data) for each pollutant besides UFP (Figure S6).

Exposure Disparities by HOLC Grade

Table 4 lists the population-weighted pollutant means by HOLC grade. Concentrations were similar between grades A and B for

UFPs, but they increased by 12% (940 pt/cm³) relative to Grade A for Grade C, 28% (2,300 pt/cm³) for Grade D, and 49% (4,600 pt/cm³) for Grade X. BC had a 12% (70 ng/m³) disparity between grades A and D, and a 48% (349 ng/m³) disparity between grades A and X, whereas NO₂ had a 26% (2.7 ppb) and 58% (7.5 ppb) disparity for Grade A compared with grades D and X, respectively. PM_{2.5} differed from the other pollutants in that its increase in concentration relative to Grade A is lowest in Grade D. For all pollutants, Grade X had the highest pollution levels.

Because the overall pollutant concentrations were higher in the HOLC-graded region in comparison with the overall study region, we conducted a sensitivity analysis for the separate race and ethnicity and income analyses reported in Tables 2 and 3 restricted to the HOLC-graded region only (Tables S5 and S6).

Table 2. Population-weighted mean pollutant concentration (2019–2020) by block-level income group (2006–2010 American Community Survey) and the percentage difference in comparison with the population-weighted average concentration of the Greater Seattle Area study region.

Income group	Population (N) ^a	UFP (pt/cm ³)	Percentage difference from average (%)	BC (ng/m ³)	Percentage difference from average (%)	NO ₂ (ppb)	Percentage difference from average (%)	PM _{2.5} (μg/m ³)	Percentage difference from average (%)
≤\$20,000	29,840	10,000	40	724	33	13.9	46	5.2	12
\$20,000–\$40,000	226,576	8,010	18	599	14	10.0	14	4.8	4
\$40,000–\$50,000	224,697	7,380	10	568	9	9.4	8	4.7	2
\$50,000–\$60,000	251,393	7,330	9	549	5	9.3	7	4.7	2
\$60,000–\$70,000	260,149	6,690	0	527	1	8.9	2	4.6	0
\$70,000–\$80,000	225,710	6,400	–4	509	–2	8.5	–2	4.6	0
\$80,000–\$90,000	207,462	5,980	–11	481	–8	8.0	–8	4.4	–4
\$90,000–\$110,000	295,690	5,550	–18	454	–14	7.6	–13	4.4	–4
>\$110,000	193,475	5,710	–16	453	–14	7.6	–13	4.3	–7
Overall population	1,914,992	6,680	—	520	—	8.7	—	4.6	—

^aPopulation numbers do not add up to the total owing to rounding.

Note: —, not applicable; BC, black carbon; NO₂, nitrogen dioxide; PM_{2.5}, fine particulate matter; pt, particles; UFP, ultrafine particles.

Table 3. Population-weighted mean pollutant concentration (2019–2020) by racial and ethnic group (2010 U.S. Census) and the percentage difference in comparison with the population-weighted average concentration of the Greater Seattle Area study region.

Group	Population [N (%)]	UFP (pt/cm ³)	Percentage difference from average (%)	BC (ng/m ³)	Percentage difference from average (%)	NO ₂ (ppb)	Percentage difference from average (%)	PM _{2.5} (µg/m ³)	Percentage difference from average (%)
Asian	293,808 (15)	6,890	3	524	1	8.8	1	4.5	-1
Black	124,656 (7)	7,740	15	566	8	9.4	7	4.7	3
Hispanic	180,656 (9)	7,060	6	535	3	8.8	1	4.6	0
Native American	14,692 (1)	7,210	8	547	5	9.2	5	4.7	3
Non-Hispanic White	1,210,551 (63)	6,450	-4	512	-2	8.6	-1	4.6	0
Pacific Islander	14,559 (1)	7,470	11	546	5	8.8	1	4.6	0
Overall population	1,914,992	6,680	—	520	—	8.7	—	4.6	—

Note: —, not applicable; BC, black carbon; NO₂, nitrogen dioxide; PM_{2.5}, fine particulate matter; pt, particles; UFP, ultrafine particles.

Although the degree of disparities was smaller, the general patterns observed in the HOLC-graded region were similar to those of the entire study region.

Table 5 shows the results of two sets of population-weighted regression analyses by pollutant within the HOLC-graded region, namely, crude models with *a*) HOLC grade alone, and *b*) HOLC grade adjusted for median household income and percentage of non-Hispanic White population. The two continuous predictors were centered as described in the “Methods” section, so the Grade A means were similar in both models. In the single-predictor models, the intercepts represent the marginal (unadjusted) population-weighted means for HOLC Grade A.

The results show a complex relationship between these three factors across all four pollutants. In the crude analysis, progressively more hazardous graded areas generally had progressively higher air pollution concentrations, with a few exceptions: There was little relationship between grade and PM_{2.5}, and slightly lower UFPs for Grade B than Grade A. Adjusting the analysis for median income and non-Hispanic White percentage attenuated most of the existing relationships for grades B and C, except that

the difference between grades B and A for UFP became more exaggerated. In contrast, the Grade D and X exposures were still substantially higher than Grade A despite the attenuation for all non-PM_{2.5} comparisons, consistent with the crude model results.

Sensitivity Analysis: HOLC-Graded Area

There were no meaningful differences between including or excluding blocks that fell under multiple grades (Table S1). The biggest difference was between average UFP exposures for Grade D, which was a 2% difference. There was no meaningful difference in weighing the population split compared with splitting it evenly either, with the results being even closer (Table S2). As shown in Table S5, the decreasing trend across income groups in the restricted redlining area is similar to the trend across the overall study area (Table 2). There is a less dramatic difference between the lowest income group and the next lowest income group in the redlining area compared with the overall study area. The median UFP concentrations of the lowest income group (<\$20,000) and the second lowest (\$20,000–\$40,000) for

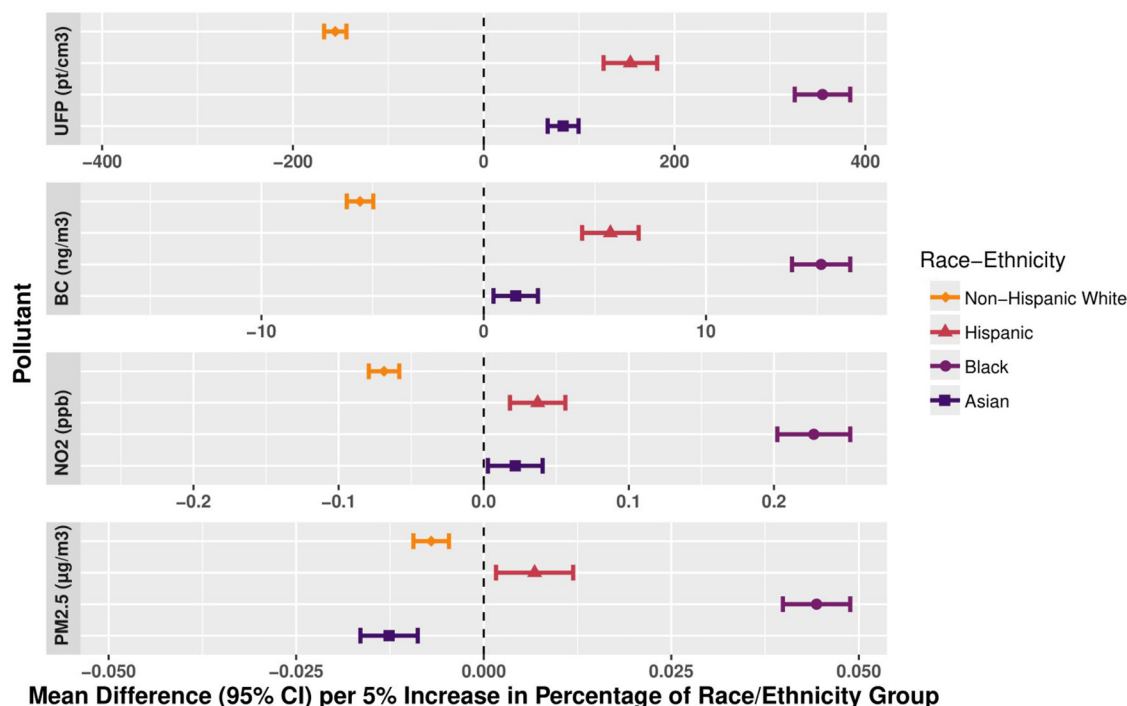


Figure 3. Mean difference (95% CI) in pollutant concentration (2019–2020) per 5% increase in percentage race and ethnicity group by census block. Point estimates are regression estimates and error bars are 95% CIs. Each group was modeled separately in population-weighted linear regression models, with the percentage of that specific racial or ethnic group, from the 2010 U.S. Census,⁴⁶ in the block as the predictor. Models accounted for spatial correlation using generalized estimating equations with identity links. Data can be found in Table S4. Note: BC, black carbon; CI, confidence interval; NO₂, nitrogen dioxide; PM_{2.5}, fine particulate matter; pt, particles; UFP, ultrafine particles.

Table 4. Population-weighted mean pollutant concentration (2019–2020) in blocks by historical Home Owners’ Loan Corporation (HOLC) redlining grade and percentage differences in comparison with HOLC Grade A in Seattle. Present-day blocks that fall between multiple grades contribute population evenly to each of those grades.

HOLC grade	Population (N)	UFP (pt/cm ³)	Percentage difference from Grade A (%)	BC (ng/m ³)	Percentage difference from Grade A (%)	NO ₂ (ppb)	Percentage difference from Grade A (%)	PM _{2.5} (µg/m ³)	Percentage difference from Grade A (%)
A	15,884	7,150	—	547	—	9.3	—	4.8	—
B	188,178	7,050	–1	576	5	10.4	12	4.9	4
C	145,150	8,090	12	618	12	10.8	15	5.1	6
D	83,986	9,450	28	617	12	12.0	26	4.8	0
X	45,343	11,750	49	896	48	16.8	58	5.6	16

Note: —, not applicable; BC, black carbon; NO₂, nitrogen dioxide; PM_{2.5}, fine particulate matter; pt, particles; UFP, ultrafine particles.

the study area were 10,000 pt/cm³ and 8,010 pt/cm³, whereas for the redlining area, they were 10,300 and 9,590 pt/cm³, respectively. This is a 22% difference between the lowest and second lowest income group for the study area, whereas it is a 7% difference for the redlining area.

As shown in Table S6, the overall pollution levels for each racial and ethnic group are higher in the redlining area compared with the same set of results compiled for the overall study area (Table 3). The average air pollution was more homogenous in the redlining area compared with the overall study area, but the UFP concentrations were still lowest for non-Hispanic White residents. There is a meaningful difference in UFP exposures for non-Hispanic White residents vs. racial and ethnic minorities, with the percentage difference for minorities relative to the overall population being between 7–9% for each group.

Discussion

The present study is one of only a few to examine UFP exposure disparities by income, race and ethnicity, and HOLC grade and to compare these with other pollutant disparities. Our findings suggest that in the Greater Seattle Area there are disparities by income, race and ethnicity, and HOLC grade for UFP, BC, NO₂, and PM_{2.5} and that those disparities are generally greatest for UFPs, regardless of how the disparities are characterized. These disparities were present even though pollutant concentrations are generally low in the Greater Seattle Area. Concentrations of all four pollutants were higher in lower-income communities than higher-income communities. In comparison with the population-weighted study region average concentration, exposure to both UFP and NO₂ was at least 40% higher on average in the lowest (<\$20,000) income group. For incomes between \$20,000 and \$60,000, UFP concentrations were 9–18% higher than the average concentration; this was the largest relative disparity across the four pollutants. In addition, historically racialized groups were exposed to higher concentrations of UFPs than non-Hispanic White residents on average. Black residents had the highest exposures across all pollutants.

Our findings are consistent with and extend previous studies that found NO₂, PM_{2.5}, O₃, and carbon monoxide concentrations to be higher for racialized people and PM to be higher in areas with lower socioeconomic status.^{5–13} We extend those findings by showing similar patterns with UFP and BC concentrations. Although the NO₂ and PM_{2.5} concentrations in our study region were lower than U.S. EPA standards, we show that disparities in these pollutants, especially in NO₂, are still present. Further, the associations for income and for each racial and ethnic group revealed larger disparities for UFPs and BC than for NO₂ and PM_{2.5}, which may lead to greater health disparities. As described above, adverse health effects due to UFP exposure may be magnified owing to the potential for UFPs to enter the bloodstream.²⁸

We additionally extended findings from previous studies on historical HOLC grade and air pollution to disparities for UFPs

and BC. Lane et al., Schuyler and Wenzel, and Kane previously found disparities by HOLC grade for PM_{2.5}, with Lane et al. finding additional disparities for NO₂, and Schuyler and Wenzel for nitrogen oxide, sulfur dioxide, and volatile organic compounds.^{31–33} We found that, in the parts of Seattle subjected to historical redlining, neighborhoods that were once characterized as hazardous were exposed to higher concentrations of UFP, BC, and NO₂ in 2019, with the largest differences apparent for HOLC Grade D. Kane additionally compared PM_{2.5} concentrations in non-HOLC-graded regions to HOLC-graded regions within county boundaries, finding higher PM_{2.5} concentrations in HOLC-graded regions.³³ We also found that concentrations of each pollutant were higher in HOLC-graded regions than non-HOLC-graded regions (Table 1; study region section). We further defined a Grade X for the interior uncategorized areas within the HOLC-graded region, which were blocks with residential populations in the 2010 U.S. Census that were deemed to be business or industrial areas in the 1930s. The elevated pollutant concentrations were the highest in the Grade X area. One reason may be that the industrial infrastructure remains and is a potential source of air pollution, despite present-day residential population. These disparities were greater than those separately observed by racial and ethnic groups, even when the race and ethnicity analysis was restricted to the HOLC-graded region (Table S6). Similar to the other studies, we first calculated average concentrations by HOLC grade, but because of the complex relationship between redlining, income, and race and ethnicity, we then additionally evaluated these associations in a multivariable analysis (Table 5). We found, after adjusting for income and non-Hispanic White population percentage, that although estimated concentrations for less desirable HOLC grades were lower, there remained statistically significant elevated pollutant concentrations in areas previously assigned Grade D and Grade X.

Our goal was to describe disparities, rather than ask causal questions. Thus, the multivariable analysis in Table 5 used regression adjustment to make comparisons of the areas assigned more hazardous grades with those assigned Grade A. Although this is not a realistic counterfactual comparison across all grades, owing to the low probability of any areas graded as hazardous receiving an A grade, it did allow us to describe how much exposures would need to decline in the groups with the highest exposures to be comparable to those with the lowest. Further, in our multivariable analyses, we were able to assess whether the observed disparities differ when we consider HOLC grade alone as compared to models that also consider modern-day income and race and ethnicity percentage. The results show that the grade-specific disparities indeed changed after adjusting for modern-day census characteristics. After adjustment for income and race and ethnicity, the disparities in grades D and X remained statistically significant for UFPs, BC, and NO₂. Although racial and economic status were significant factors in assigning HOLC grades, other factors, such as industrial presence, were higher in

Table 5. Population-weighted mean pollutant estimates (95% CIs) from regression models with Home Owners' Loan Corporation (HOLC) redlining grade as predictor variable, alone and after adjustment for log₁₀-transformed median household income (2006–2010 American Community Survey) and non-Hispanic White population percentage (2010 U.S. Census) in the Greater Seattle Area.

Pollutant	Regression type	Mean pollutant estimate (95% CI)						
		Grade A mean	Median household income (\$10,000 increase)	Non-Hispanic White population (10% increase)	Grade B difference	Grade C difference	Grade D difference	Grade X difference
UFP (pt/cm ³)	Crude	7,150 (7,060, 7,230)	—	—	-101 (-197, -6)	937 (832, 1,043)	2,305 (2,135, 2,476)	4,599 (4,321, 4,877)
	Adjusted	7,170 (7,080, 7,250)	-43 (-54, -32)	-179 (-201, -158)	-485 (-588, -383)	61 (-68, 189)	1,216 (1,022, 1,409)	3,719 (3,431, 4,007)
BC (ng/m ³)	Crude	547.2 (541.5, 553.0)	—	—	28.9 (21.4, 36.3)	71.1 (63.1, 79.2)	69.6 (57.8, 81.4)	349.1 (335.7, 362.6)
	Adjusted	549.4 (543.5, 555.3)	-4.6 (-5.4, -3.8)	1.7 (0.1, 3.2)	3.0 (-4.6, 10.6)	38.2 (27.7, 48.8)	31.8 (18.0, 45.6)	299.9 (284.2, 315.6)
NO ₂ (ppb)	Crude	9.29 (9.19, 9.39)	—	—	1.14 (1.01, 1.28)	1.52 (1.38, 1.66)	2.76 (2.46, 3.05)	7.52 (7.15, 7.88)
	Adjusted	9.35 (9.25, 9.46)	-0.14 (-0.16, -0.12)	0.10 (0.06, 0.13)	0.40 (0.25, 0.55)	0.66 (0.45, 0.87)	1.79 (1.47, 2.10)	6.13 (5.71, 6.55)
PM _{2.5} (µg/m ³)	Crude	4.75 (4.71, 4.78)	—	—	0.19 (0.15, 0.22)	0.31 (0.27, 0.35)	0.00 (-0.04, 0.05)	0.84 (0.79, 0.89)
	Adjusted	4.75 (4.72, 4.79)	-0.01 (-0.01, -0.01)	0.03 (0.03, 0.04)	0.14 (0.10, 0.18)	0.31 (0.26, 0.35)	0.02 (-0.03, 0.06)	0.78 (0.72, 0.83)

Note: Adjusted model includes all terms simultaneously and mean pollutant estimates are conditional on the other terms. —, not applicable; BC, black carbon; CI, confidence interval; NO₂, nitrogen dioxide; PM_{2.5}, fine particulate matter; pt, particles; UFP, ultrafine particles.

areas graded D and ungraded areas (Grade X), which may have contributed to our findings.²⁰ In the 1950s and 1960s, local governments across the country zoned Black neighborhoods to permit industrial activity but did not allow industry in White communities.²⁶ Furthermore, decades of disinvestment in Black neighborhoods likely contributed to the exposure disparities we observed. We continue to see the legacy of redlining in Seattle today, with lower average incomes, higher proportions of racialized groups, and overall higher pollutant concentrations in formerly redlined areas.

Schuyler and Wenzel and Kane both additionally compared pollution exposures to asthma prevalence in their study regions, finding a higher prevalence of asthma associated with lower HOLC grades in Pittsburgh, Chicago, and Dallas-Fort Worth.^{32,33} Given that our study region was confined to the Greater Seattle Area, it is noteworthy that our overall results aligned with previous research on air pollution exposure disparities. However, there may be specific features of these data and this region, such as lower variation of PM_{2.5} and lower levels of pollution overall, that differ from those observed in other locations and result in different spatial patterns. Despite the lower levels of air pollutants, disparities were still apparent in the Greater Seattle study region. Prior studies on PM_{2.5} were also able to leverage consistent long-term monitoring data, which is not yet readily available for UFPs. It will be important to study changes in UFP exposure and disparities over time, and the associated health effects.

This study offers important strengths. The air pollution data we used are a unique resource with multiple pollutants collected simultaneously and modeled by the same study, thus strengthening the cross-pollutant comparisons. They were collected by a mobile monitoring campaign that was designed to produce unbiased estimates of annual average air pollutants, without needing to adjust for short-term temporal trends as is commonly incorporated into mobile monitoring study estimates, and to target residential rather than on-road exposures. Although some studies use fixed site locations, many mobile monitoring studies collect data only while the vehicle is moving (nonstationary sampling), and thus the measurements and predictions represent on-road exposures.^{49–51} Because the Seattle mobile monitoring study used stationary sampling, where the vehicle stopped by pulling off or to the side of the road to sample for 2 min, its measurements more closely approximate off-road concentrations. Furthermore, the 309 stop locations were selected to represent residences of the target cohort, so that the predictions obtained from this study are likely to represent residential exposures and to be relevant for epidemiology, whereas the number of sites allowed us to maximize spatial coverage.

The instrumentation and mobile monitoring approach used to obtain the pollutant data in this study has both strengths and weaknesses. Our mobile monitoring study annual averages were derived from ~29 measurements totaling an hour's worth of data at each stop, which we modeled to predict annual averages at census block centroids.⁴⁴ This study was not designed to characterize the spatiotemporal nature of the variation in pollution concentrations, and these averages are noisier than those from long-term fixed site monitoring would be. In spite of the short total monitoring duration at each location, mobile monitoring studies are a useful approach for characterizing long-term average exposure to traffic-related air pollutants.^{50,52–54} This is particularly true for UFPs owing to the expense and practical challenges of measuring them and their spatial and temporal heterogeneity.⁵⁵ We contrast this with PM_{2.5}, a more regional and less spatially heterogeneous pollutant, which is not typically measured in a mobile campaign. Our PM_{2.5} exposure data were challenged additionally by low ambient levels close to the

instrument limit of detection. These pollutant and measurement features were reflected in our data set where UFPs had the largest relative spatial variability and PM_{2.5} the smallest.

Other limitations pertain to the demographic data. The years of the ACS and U.S. Census data (2006–2010) do not directly align with the exposure years (2019–2020). At the time of the mobile monitoring study, the 2020 U.S. Census data were not yet available, and predictions were made at block centroids following the 2010 U.S. Census geographies. Although ideally our exposure period and demographic data would align, we wanted to conduct our analysis at the finest scale possible, and even though more recent ACS data (2015–2019) are available, these data are only at the block group level and not the block level. Block-level data permits better small-scale spatial matching to the HOLC areas than block group data and thus more accurate population-weighted exposure averages. Although there was no historical, long-term source of UFP monitoring data in Seattle, Wang et al. documented that modeled spatial surfaces of traffic-related pollutants are stable over a 7-y period, so the temporal misalignment of the demographic and pollutant data should have minimal impact on these results.⁵⁶ Other researchers have found that although PM_{2.5} levels have widely decreased throughout the country over the decades, relative exposure disparities have remained.⁴ We hope that our study will contribute to future research to learn whether and how disparities might change for UFP once more long-term and widespread data are available. In addition, there is the potential for uncertainty in the census data itself, given that low-income neighborhoods have been shown to have higher variation in data than high-income neighborhoods.⁵⁷ Another limitation is that our classification of race and ethnicity was dependent on census classifications. The census limited our analyses to the groups (Asian, Black, Hispanic, Native American, non-Hispanic White, and Pacific Islander) that we studied. We would have liked to disaggregate the data further to, for example, examine Native American and Pacific Islander populations in our regression analyses as well but, unfortunately, the small population sizes did not allow this. Native American and Pacific Islander populations tend to suffer disproportionately from poor health outcomes and have at times been excluded from public health data collection.⁵⁸ Also owing to small population counts, we did not separately divide any groups other than White into Hispanic and non-Hispanic subsets. The degree of overlap of the Hispanic with the non-White groups was small such that the impact on our results should be minimal. Last, we were unable to disentangle the causal effects of the associations of exposure disparities. Structural racism has had broad and enduring effects on human health and exposure. A full understanding of its impacts needs to extend well beyond documentation of exposure disparities.

Overall, this study allows a comparison of disparities in exposure across both criteria air pollutants (NO₂ and PM_{2.5}) and less commonly measured air pollutants (UFPs, BC) that were obtained simultaneously from a mobile monitoring study. Racialized communities, lower-income communities, and historically redlined neighborhoods in the Seattle area were exposed to higher concentrations of UFPs, BC, NO₂, and PM_{2.5}. Concentrations were highest for the lowest income group (<\$20,000 per household/y) across all pollutants. Further, we observed large disparities by race and ethnicity, especially for Black residents, and by redlining grade for UFP, BC, and NO₂. Disparities were largest for UFP and weakest for PM_{2.5}. This multipollutant comparison is valuable for putting the results of our study into context with previous studies, most of which have focused on NO₂ and PM_{2.5}. The presence of higher exposure disparities for UFPs reinforces the need for more long-term monitoring and research on the health effects of UFPs, which will in turn guide regulation of these particles. Promoting

cleaner air will help those disproportionately exposed to air pollution and suffering from its resulting health effects.

Acknowledgments

This research was supported by award numbers R01ES026187, T32ES015459, and 1R25ES025503 from the National Institutes of Health (NIH)/National Institute of Environmental Health Sciences, and CR-83998101 from the Health Effects Institute (HEI) (all to L.S.). This content is solely the responsibility of the authors and does not necessarily represent the official views of the NIH or HEI. The corresponding code repository for this manuscript can be found at <https://github.com/kayabramble/SeattleAirPollutionDisparities>.

References

1. U.S. EPA (U.S. Environmental Protection Agency). 2019. Integrated Science Assessment (ISA) for Particulate Matter (Final Report, Dec 2019). EPA/600/R-19/188. <https://cfpub.epa.gov/ncea/isa/recordisplay.cfm?deid=347534> [accessed 8 October 2022].
2. U.S. EPA. 2016. Integrated Science Assessment (ISA) for Oxides of Nitrogen—Health Criteria (Final Report, Jan 2016). EPA/600/R-15/068. <https://cfpub.epa.gov/ncea/isa/recordisplay.cfm?deid=310879> [accessed 8 October 2022].
3. U.S. EPA. 2020. Integrated Science Assessment (ISA) for Ozone and Related Photochemical Oxidants (Final Report, Apr 2020). EPA/600/R-20/012. <https://cfpub.epa.gov/ncea/isa/recordisplay.cfm?deid=348522> [accessed 8 October 2022].
4. Colmer J, Hardman I, Shimshack J, Voorheis J. 2020. Disparities in PM_{2.5} air pollution in the United States. *Science* 369(6503):575–578, PMID: 32732425, <https://doi.org/10.1126/science.aaz9353>.
5. Chambliss SE, Pinon CPR, Messier KP, LaFranchi B, Upperman CR, Lunden MM, et al. 2021. Local- and regional-scale racial and ethnic disparities in air pollution determined by long-term mobile monitoring. *Proc Natl Acad Sci USA* 118(37):e2109249118, PMID: 34493674, <https://doi.org/10.1073/pnas.2109249118>.
6. Saha PK, Presto AA, Hankey S, Marshall JD, Robinson AL. 2022. Racial-ethnic exposure disparities to airborne ultrafine particles in the United States. *Environ Res Lett* 17(10):104047, <https://doi.org/10.1088/1748-9326/ac95af>.
7. Liu J, Clark LP, Bechle MJ, Hajat A, Kim SY, Robinson AL, et al. 2021. Disparities in air pollution exposure in the United States by race/ethnicity and income, 1990–2010. *Environ Health Perspect* 129(12):127005, PMID: 34908495, <https://doi.org/10.1289/EHP8584>.
8. Clark LP, Millet DB, Marshall JD. 2017. Changes in transportation-related air pollution exposures by race-ethnicity and socioeconomic status: outdoor nitrogen dioxide in the United States in 2000 and 2010. *Environ Health Perspect* 125(9):097012, PMID: 28930515, <https://doi.org/10.1289/EHP959>.
9. Gray SC, Edwards SE, Miranda ML. 2013. Race, socioeconomic status, and air pollution exposure in North Carolina. *Environ Res* 126:152–158, PMID: 23850144, <https://doi.org/10.1016/j.envres.2013.06.005>.
10. Brochu PJ, Yanosky JD, Paciorek CJ, Schwartz J, Chen JT, Herrick RF, et al. 2011. Particulate air pollution and socioeconomic position in rural and urban areas of the Northeastern United States. *Am J Public Health* 101(suppl 1):S224–S230, PMID: 21836114, <https://doi.org/10.2105/AJPH.2011.300232>.
11. Hajat A, Diez-Roux AV, Adar SD, Auchincloss AH, Lovasi GS, O'Neill MS, et al. 2013. Air pollution and individual and neighborhood socioeconomic status: evidence from the Multi-Ethnic Study of Atherosclerosis (MESA). *Environ Health Perspect* 121(11–12):1325–1333, PMID: 24076625, <https://doi.org/10.1289/ehp.1206337>.
12. Jbaily A, Zhou X, Liu J, Lee TH, Kamareddine L, Verguet S, et al. 2022. Air pollution exposure disparities across US population and income groups. *Nature* 601(7892):228–233, PMID: 35022594, <https://doi.org/10.1038/s41586-021-04190-y>.
13. Bell ML, Ebisu K. 2012. Environmental inequality in exposures to airborne particulate matter components in the United States. *Environ Health Perspect* 120(12):1699–1704, PMID: 22889745, <https://doi.org/10.1289/ehp.1205201>.
14. Agency for Healthcare Research and Quality. 2021. 2019 National Healthcare Quality and Disparities Report. Last reviewed June 2021. <https://www.ahrq.gov/research/findings/nhqrdr/nhqrdr19/index.html> [accessed 8 October 2022].
15. GBD US Health Disparities Collaborators. 2022. Life expectancy by county, race, and ethnicity in the USA, 2000–19: a systematic analysis of health disparities. *Lancet* 400(10345):25–38, PMID: 35717994, [https://doi.org/10.1016/S0140-6736\(22\)00876-5](https://doi.org/10.1016/S0140-6736(22)00876-5).
16. De Ramos IP, Auchincloss AH, Bilal U. 2022. Exploring inequalities in life expectancy and lifespan variation by race/ethnicity and urbanicity in the United States: 1990 to 2019. *SSM Popul Health* 19:101230, PMID: 36148325, <https://doi.org/10.1016/j.ssmph.2022.101230>.

17. Chetty R, Stepner M, Abraham S, Lin S, Scuderi B, Turner N, et al. 2016. The association between income and life expectancy in the United States, 2001–2014. *JAMA* 315(16):1750–1766, PMID: 27063997, <https://doi.org/10.1001/jama.2016.4226>.
18. National Academy of Sciences. 2017. Communities in Action: Pathways to Health Equity. <https://nap.nationalacademies.org/resource/24624/TransportationforHealthEquity/> [accessed 8 October 2022].
19. Dwyer-Lindgren L, Bertozzi-Villa A, Stubbs RW, Morozoff C, Mackenbach JP, van Lenthe FJ, et al. 2017. Inequalities in life expectancy among US counties, 1980 to 2014: temporal trends and key drivers. *JAMA Intern Med* 177(7):1003–1011, PMID: 28492829, <https://doi.org/10.1001/jamainternmed.2017.0918>.
20. Mitchell B, Franco J. 2018. National Community Reinvestment Coalition. HOLC “redlining” maps: the persistent structure of segregation and economic inequality. <https://ncrc.org/holc/> [accessed 8 October 2022].
21. Nelson RK, Winling L, Marciano R, Connolly N, et al. n.d. American Panorama. Mapping Inequality. <https://dsi.richmond.edu/panorama/redlining/#loc=5/39.1/-94.58> [accessed 8 October 2022].
22. White AG, Guikema SD, Logan TM. 2021. Urban population characteristics and their correlation with historic discriminatory housing practices. *Appl Geogr* 132:102445, <https://doi.org/10.1016/j.apgeog.2021.102445>.
23. Richardson J, Mitchell BC, Meier HCS, Lynch E, Edlebi J, Nelson RK, et al. 2020. National Community Reinvestment Coalition. Redlining and neighborhood health. <https://ncrc.org/holc-health/> [accessed 8 October 2022].
24. Nardone A, Rudolph KE, Morello-Frosch R, Casey JA. 2021. Redlines and greenspace: the relationship between historical redlining and 2010 greenspace across the United States. *Environ Health Perspect* 129(1):017006, PMID: 33502254, <https://doi.org/10.1289/EHP7495>.
25. Swope CB, Hernández D, Cushing LJ. 2022. The relationship of historical redlining with present-day neighborhood environmental and health outcomes: a scoping review and conceptual model. *J Urban Health* 99(6):959–983, PMID: 35915192, <https://doi.org/10.1007/s11524-022-00665-z>.
26. Rothstein R. 2017. *The Color of Law: A Forgotten History of How Our Government Segregated America*. 1st ed. New York, NY: Liveright Publishing Corporation.
27. Arcaya MC, Figueroa JF. 2017. Emerging trends could exacerbate health inequities in the United States. *Health Aff (Millwood)* 36(6):992–998, PMID: 28583956, <https://doi.org/10.1377/hlthaff.2017.0011>.
28. Terzano C, Di Stefano F, Conti V, Graziani E, Petrianni A. 2010. Air pollution ultrafine particles: toxicity beyond the lung. *Eur Rev Med Pharmacol Sci* 14(10):809–821, PMID: 21222367.
29. Schraufnagel DE. 2020. The health effects of ultrafine particles. *Exp Mol Med* 52(3):311–317, PMID: 32203102, <https://doi.org/10.1038/s12276-020-0403-3>.
30. Kwon HS, Ryu MH, Carlsten C. 2020. Ultrafine particles: unique physicochemical properties relevant to health and disease. *Exp Mol Med* 52(3):318–328, PMID: 32203103, <https://doi.org/10.1038/s12276-020-0405-1>.
31. Lane HM, Morello-Frosch R, Marshall JD, Apte JS. 2022. Historical redlining is associated with present-day air pollution disparities in U.S. cities. *Environ Sci Technol Lett* 9(4):345–350, PMID: 35434171, <https://doi.org/10.1021/acs.estlett.1c01012>.
32. Schuyler AJ, Wenzel SE. 2022. Historical redlining impacts contemporary environmental and asthma-related outcomes in Black adults. *Am J Respir Crit Care Med* 206(7):824–837, PMID: 35612914, <https://doi.org/10.1164/rccm.202112-27070C>.
33. Kane CEM. 2022. *Disparate Exposure to Fine Particulate Air Pollution in Formerly Redlined Cities: Chicago, Dallas, and Fort Worth*. Master’s thesis. Austin, TX: University of Texas at Austin.
34. Hwa Jung K, Pitkowsky Z, Argenio K, Quinn JW, Bruzzese JM, Miller RL, et al. 2022. The effects of the historical practice of residential redlining in the United States on recent temporal trends of air pollution near New York City schools. *Environ Int* 169:107551, PMID: 36183489, <https://doi.org/10.1016/j.envint.2022.107551>.
35. Nardone A, Chiang J, Corburn J. 2020. Historic redlining and urban health today in U.S. cities. *Environ Justice* 13(4):109–119, <https://doi.org/10.1089/env.2020.0011>.
36. Namin S, Xu W, Zhou Y, Beyer K. 2020. The legacy of the Home Owners’ Loan Corporation and the political ecology of urban trees and air pollution in the United States. *Soc Sci Med* 246:112758, PMID: 31884239, <https://doi.org/10.1016/j.socscimed.2019.112758>.
37. Nardone A, Casey JA, Morello-Frosch R, Mujahid M, Balmes JR, Thakur N. 2020. Associations between historical residential redlining and current age-adjusted rates of emergency department visits due to asthma across eight cities in California: an ecological study. *Lancet Planet Health* 4(1):E24–E31, PMID: 31999951, [https://doi.org/10.1016/S2542-5196\(19\)30241-4](https://doi.org/10.1016/S2542-5196(19)30241-4).
38. Clean Air Act Amendments of 1990. 1990. Pub L 101-549. <https://www.congress.gov/bill/101st-congress/senate-bill/1630/text> [accessed 19 June 2023].
39. U.S. EPA. 2022. Air data basic information. Last updated 13 October 2022. <https://www.epa.gov/outdoor-air-quality-data/air-data-basic-information> [accessed 9 October 2022].
40. Presto AA, Saha PK, Robinson AL. 2021. Past, present, and future of ultrafine particle exposures in North America. *Atmos Environ* 10:100109, <https://doi.org/10.1016/j.aea.2021.100109>.
41. Janssen NAH, Hoek G, Simic-Lawson M, Fischer P, van Bree L, ten Brink H, et al. 2011. Black carbon as an additional indicator of the adverse health effects of airborne particles compared with PM₁₀ and PM_{2.5}. *Environ Health Perspect* 119(12):1691–1699, PMID: 21810552, <https://doi.org/10.1289/ehp.1003369>.
42. Paunescu AC, Casas M, Ferrero A, Pañella P, Bougas N, Beydon N, et al. 2019. Associations of black carbon with lung function and airway inflammation in schoolchildren. *Environ Int* 131:104984, PMID: 31301585, <https://doi.org/10.1016/j.envint.2019.104984>.
43. Pun VC, Ho KF. 2019. Blood pressure and pulmonary health effects of ozone and black carbon exposure in young adult runners. *Sci Total Environ* 657:1–6, PMID: 30530214, <https://doi.org/10.1016/j.scitotenv.2018.11.465>.
44. Blanco MN, Gasset A, Gould T, Doubleday A, Slager DL, Austin E, et al. 2022. Characterization of annual average traffic-related air pollution concentrations in the Greater Seattle Area from a year-long mobile monitoring campaign. *Environ Sci Technol* 56(16):11460–11472, PMID: 35917479, <https://doi.org/10.1021/acs.est.2c01077>.
45. U.S. Census Bureau. 2021. 2006–2010 ACS 5-year Estimates. <https://www.census.gov/programs-surveys/acs/technical-documentation/table-and-geography-changes/2010/5-year.html> [accessed 21 June 2023].
46. U.S. Census Bureau. n.d. Year 2010 Summary File 1 Dataset. https://www2.census.gov/geo/tiger/TIGER2010BLKPOP/PHU/tabblock2010_53_pophu.zip [accessed 22 May 2015].
47. Hui FK, Bondell HD. 2022. Spatial confounding in generalized estimating equations. *Am Stat* 76(3):238–247, <https://doi.org/10.1080/00031305.2021.2009372>.
48. U.S. EPA. 2022. NAAQS Table. <https://www.epa.gov/criteria-air-pollutants/naaqs-table> [accessed 9 October 2022].
49. Hankey S, Marshall JD. 2015. Land use regression models of on-road particulate air pollution (particle number, black carbon, PM_{2.5}, particle size) using mobile monitoring. *Environ Sci Technol* 49(15):9194–9202, PMID: 26134458, <https://doi.org/10.1021/acs.est.5b01209>.
50. Messier KP, Chambliss SE, Gani S, Alvarez R, Brauer M, Choi JJ, et al. 2018. Mapping air pollution with Google Street View Cars: efficient approaches with mobile monitoring and land use regression. *Environ Sci Technol* 52(21):12563–12572, PMID: 30354135, <https://doi.org/10.1021/acs.est.8b03395>.
51. Weichenthal S, Ryswyk KV, Goldstein A, Shekarrizfard M, Hatzopoulou M. 2016. Characterizing the spatial distribution of ambient ultrafine particles in Toronto, Canada: a land use regression model. *Environ Pollut* 208(pt A):241–248, PMID: 25935348, <https://doi.org/10.1016/j.envpol.2015.04.011>.
52. Saha PK, Li HZ, Apte JS, Robinson AL, Presto AA. 2019. Urban ultrafine particle exposure assessment with land-use regression: influence of sampling strategy. *Environ Sci Technol* 53(13):7326–7336, PMID: 31150214, <https://doi.org/10.1021/acs.est.9b02086>.
53. Hatzopoulou M, Valois MF, Levy I, Mihele C, Lu G, Bagg S, et al. 2017. Robustness of land-use regression models developed from mobile air pollutant measurements. *Environ Sci Technol* 51(7):3938–3947, PMID: 28241115, <https://doi.org/10.1021/acs.est.7b00366>.
54. Blanco MN, Doubleday A, Austin E, Marshall JD, Seto E, Larson TV, et al. 2023. Design and evaluation of short-term monitoring campaigns for long-term air pollution exposure assessment. *J Expo Sci Environ Epidemiol* 33(3):465–473, PMID: 36045136, <https://doi.org/10.1038/s41370-022-00470-5>.
55. Brugge D, Fuller CH. 2021. *Ambient Combustion Ultrafine Particles and Health*. 1st ed. Hauppauge, NY: Nova Science Publishers.
56. Wang R, Henderson SB, Sbihi H, Allen RW, Brauer M. 2013. Temporal stability of land use regression models for traffic-related air pollution. *Atmos Environ* 64:312–319, <https://doi.org/10.1016/j.atmosenv.2012.09.056>.
57. Folch DC, Arribas-Bel D, Koschinsky J, Spielman SE. 2016. Spatial variation in the quality of American Community Survey estimates. *Demography* 53(5):1535–1554, PMID: 27541024, <https://doi.org/10.1007/s13524-016-0499-1>.
58. Urban Indian Health Institute. 2022. Data genocide of American Indians and Alaska Natives in COVID-19 data. <https://www.uihi.org/projects/data-genocide-of-american-indians-and-alaska-natives-in-covid-19-data> [accessed 9 October 2022].